Arabian Journal of Chemistry (2022) **15**, 104289

King Saud University

Arabian Journal of Chemistry

www.ksu.edu.sa
www.sciencedirect.com

ORIGINAL ARTICLE

Oxidation reaction and thermal stability of 1,3-butadiene under oxygen and initiator

Min Liang, Huixia Zhao, Suyi Dai, Chang Yu, Haijun Cheng, Weiguang Li, Fang Lai, Li Ma *, Xiongmin Liu *

School of Chemistry and Chemical Engineering, Guangxi University, Nanning 530004, China

Received 9 May 2022; accepted 18 September 2022
Available online 22 September 2022

KEYWORDS

1,3-Butadiene;
Thermal oxidation;
Initiator;
Peroxide;
DSC

Abstract 1,3-Butadiene is the simplest conjugated diene, which is widely used in polymer materials, organic synthesis, and other fields. The investigation of its thermal stability and oxidation characteristics is necessary for production, transportation, and use safety. The pressure and temperature behavior of the autoxidation reaction of 1,3-butadiene with oxygen were determined using a custom-designed mini closed pressure vessel test (MCPVT). The effects of free radical initiators CHP and AIBN on the oxidation reaction were investigated. The thermal decomposition characteristics of oxidation products were measured by differential scanning calorimetry (DSC), and its hazards were discussed. The results showed that the oxidation reaction of 1,3-butadiene was easy to occur. Moreover, the activation energies of autoxidation, CHP-initiated oxidation, and AIBN-initiated oxidation reaction were 20.85 kJ·mol^{-1}, 33.30 kJ·mol^{-1}, and 56.27 kJ·mol^{-1}, respectively. In addition, the oxidation products were analyzed by headspace sampler-gas chromatography-mass spectrometry (HS-GC–MS), GC–MS, and iodometry. Some of 1,3-butadiene oxidation products under three conditions are the same, for example, 3-butene-1,2-diol, 4-vinylcyclohexene, 2(5H)-furanone, 2-propen-1-ol, and 2,6-cyclooctadien-1-ol. According to the reaction products, the oxidation reaction pathway of 1,3-butadiene was described. The research results are significant for avoiding fire and explosion accidents in the production, transportation, and application of 1,3-butadiene.

1. Introduction

1,3-Butadiene is a simple conjugated diene that is ubiquitously used as a significant component of manufactured rubber, resins, and plastics in the chemical industry (Dai et al., 2019; Dias et al., 2019; Bonnevide et al., 2020). It has been a detailed examination of its thermostability and polymerization properties. There is increasing controversy about the beneficial effects of 1,3-butadiene in general, with questions about their benefits as necessary basic chemical raw materials versus risks as a flammable and combustible material. In the presence of oxygen, rust, carbonyl, and other substances, it is easy to form popcorn-like poly-

* Corresponding authors.
E-mail addresses: gxumali@126.com (L. Ma), xmliu1@gxu.edu.cn (X. Liu).
Peer review under responsibility of King Saud University.

Production and hosting by Elsevier

https://doi.org/10.1016/j.arabjc.2022.104289

mers such as end-group polymers and peroxide polymers. Under suitable conditions, popcorn-like polymers are prone to a chain reaction, resulting in a chemical explosion (Alexander, 1959; Klais, 1993). From a safety point of view, it is essential to understand its behavior concerning oxidation because its production, storage, and usage are complicated by autoxidation and the resulting formation of 1,3-butadiene polyperoxide (Liu et al., 2020).

Kinetics, products, and mechanism of 1,3-butadiene oxidation under the initiation of OH and other oxidizing conditions (including O_3, high temperature, microbial, catalysis, and radical generator AIBN) have been reported in many literatures (Cavani et al., 1983; Adusei and Fontijn, 1993; Li et al., 2006a,b; Ghosh et al., 2010a,b; Vasu et al., 2010). Specifically, Brezinsky et al. studied the oxidation and pyrolysis of 1,3-butadiene in an atmospheric flow reactor at approximately 1100 K. They revealed that the oxidation of 1,3-butadiene occurs through O atom addition to the double bond (Brezinsky et al., 1985). Laskin et al. examined the high-temperature kinetics of 1,3-butadiene oxidation with a detailed kinetic model. They determined the most critical channel as the chemical-activated reaction of H· and 1,3-butadiene to produce the vinyl radical (Lifshitz and Laskin, 1994). Kramp et al. studied the gas-phase reaction of ozone with 1,3-butadiene at room temperature and pressure and measured the yields of acrolein, 1,2-epoxy-3-butene, and OH radicals (Kramp and Paulson, 2000). Li et al. researched the kinetics of the reaction of hydroxyl radical with 1,3-butadiene at 240–340 K and a total pressure of 1 Torr using a relative rate combined with the discharge flow and mass spectrometer technique (Li et al., 2006a,b). Ghosh et al. reported the first isomeric selective kinetic study of the dominant isomeric pathway in the OH-initiated oxidation of 1,3-butadiene in the presence of O_2 and NO (Ghosh et al., 2010a,b). Hendry et al. investigated the liquid-phase oxidation of 1,3-butadiene at 313.15 and 323.15 K by adding 2,2′-azobisisobutyronitrile (AIBN) as an initiator (Hendry et al., 1968a,b). The result showed that the rate was constant in the presence of AIBN, without an induction period or autocatalysis. It was fresh and particular that AIBN acts as an initiator of oxidation because initiators are often considered to be used in radical polymerizations of organic compounds (Denisov et al., 2003; Wang et al., 2016; Yamamoto and Takahashi, 2016). There are some examples of using initiators in the oxidation process, such as using *tert*-butyl hydroperoxide (TBHP)(Feng and Zeng, 2020) and cumene hydroperoxide (CHP)(Safa and Ma, 2015).

For 1,3-butadiene, the initiator plays a vital role in the polymerization reaction and is mainly used in synthesizing and processing polybutadiene rubber (Huang and Sundberg, 1995; Paz-Pazos and Pugh, 2005; Abdollahi and Hajiataloo, 2021). Organic peroxide, azo compounds, and oxidation reductants can be used as initiators in the industry. Important industrial initiators include benzoyl peroxide (BPO), di-*tert*-butyl peroxide (DTBP), CHP, TBHP, AIBN, and so on (Guilun et al., 2013). The initiator was easy to cleave homogeneously at the weak bond to form two free radicals, which were very active and tried to stabilize by abstracting electrons from nearby molecules (Denisov et al., 2003). It could have an automatic acceleration effect (Guilun et al., 2013). So, whether the presence of initiators can promote the reaction between 1,3-butadiene and oxygen and thus affect the safety of the polymerization of 1,3-butadiene initiated by initiators is an issue needed concern. There has not been any systematic study on the effect of 1,3-butadiene oxidation initiated by the initiator. It is also unclear whether one mode of oxidative transformation is preferred based on the conditions of different initiators. Therefore, in this work, AIBN was used as an azo-free radical initiator according to prior literature procedures (Hendry et al., 1968a,b), and organic peroxide CHP was used to initiate the oxidation of 1,3-butadiene.

In this paper, the oxidation reaction and thermal stability of 1,3-butadiene under oxygen and two initiators CHP and AIBN were investigated by a mini closed pressure vessel test (MCPVT). The central aim of this study is to systematically examine how the similarities and differences of 1,3-butadiene oxidation can be affected by the nature of the oxidation systems. The kinetics of oxidation reactions has been investigated at low temperature for three different oxidation models. The oxidation products were analyzed by headspace sampler-gas chromatography-mass spectrometry (HS-GC–MS) and GC–MS. The thermal characteristics of oxidation products were determined via differential scanning calorimeter (DSC) techniques. This study provides a deeper insight into the underlying mechanism involved in the oxidation process. It can also explain the effect of oxygen on the production process of 1,3-butadiene polymerization using an initiator.

2. Experimental

2.1. Materials

1,3-Butadiene (mass purity > 99.90 %, molecular weight 54.09 g·mol^{-1}) was obtained from Guangdong Walter Gas Co., ltd., China. 2,2′-Azobisisobutyronitrile (AIBN) (98 % Shanghai Macklin Biochemical Co., ltd, China), cumyl hydroperoxide (CHP) (≥80 %, Aladdin Industrial Corporation, China), N_2, O_2 (99.99 %, Nanning Zhong Yi Chuang Gas Co., ltd, China), KI (99.50 %, Aladdin Industrial Corporation, China), and $Na_2S_2O_3$ (99.95 %, Aladdin Industrial Corporation, China) were used in the experiments.

2.2. Thermal oxidation of 1,3-butadiene by MCPVT

Based on the pressure vessel test (PVT, an experimental method used by the United Nations Specialized Committee on Dangerous Goods to assess the intensity of decomposition of chemical hazards) (Okada et al., 2014), a mini closed pressure vessel test (MCPVT, vessel volume: 25 mL) system was designed to measure the change of pressure (P) and temperature (T) during the decomposition of chemicals hazards. The experimental device comprises four parts: a mini closed pressure container, a temperature control system, a pressure/temperature sensor, and a pressure/temperature recorder, as shown in Fig. 1. The thermal oxidation reaction of 1,3-butadiene was evaluated by monitoring the T and P behaviors of the container. The amount of substance was calculated with the ideal gas equation (PV = nRT) to monitor the decomposition reaction. An internal glass bottle (3 mL) was settled into the stainless-steel vessel as a sampling container. The sample mass of 1,3-butadiene is 0.33 g, and the initial pressure of oxygen delivered from the gas cylinder to the container through the intake valve was set to 0.6 MPa. The autoxidation reaction in pure 1,3-butadiene without an initiator was performed at first. Then, about a 2 % mass fraction of the initiators, CHP and AIBN, were used to initiate the oxidation of 1,3-butadiene for the other two types of oxidation models. Isothermal experiments were conducted at 323–363 K for 8 h in an oxygen atmosphere. When the reactor was heated, the inner temperature and pressure were changed and recorded by the recorder and signal processor. After the reaction, the reactor was cooled to room temperature in a cold-water bath. The products were collected and analyzed.

2.3. Analysis of 1,3-butadiene peroxide by iodimetry

Peroxide was both impact-sensitive and thermally unstable. It is of paramount importance to determine the peroxide content of 1,3-butadiene by iodimetry at different temperatures. Several oxidation products were dissolved in potassium iodide-

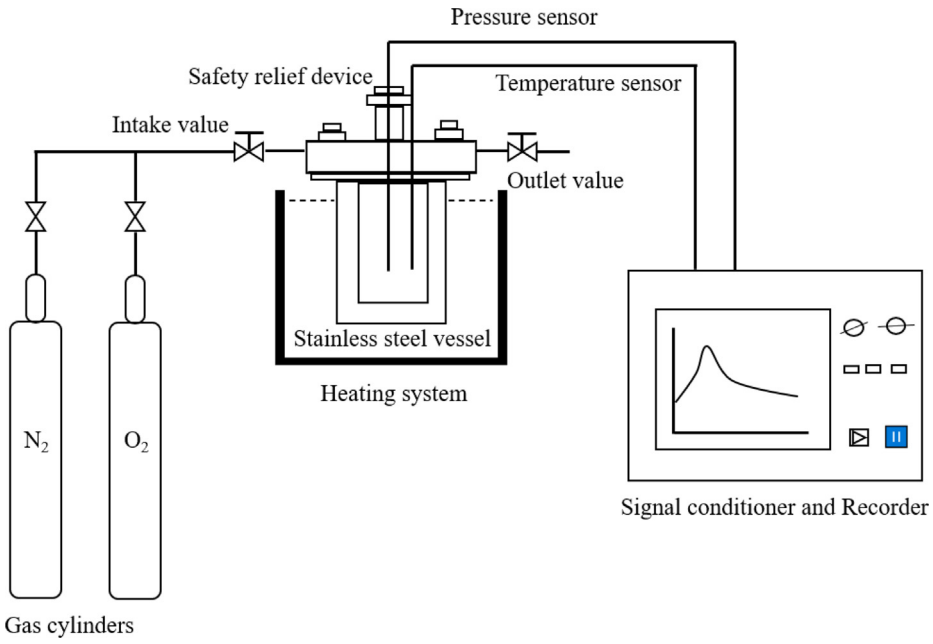

Fig. 1 The reaction device of 1,3-butadiene oxidation.

starch solution. The generated peroxides oxidized the potassium iodide to an equivalent amount of iodine (Eq. (1)). The iodine molecules were linked with starch to form a complex, which turned the solution blue. Then, the standardized sodium thiosulfate solution was used to titrate the blue solution for the end of the color disappeared (Eq. (2)). The results were quantified as milligrams per kilogram (mmol·kg^{-1}) of peroxide.

$$2KI + ROOH + H_2O \rightarrow I_2 + 2KOH + ROH \quad (1)$$

$$I_2 + 2Na_2S_2O_3 \rightarrow Na_2S_4O_6 + 2NaI \quad (2)$$

2.4. Differential scanning calorimetry (DSC)

Dynamic scanning experiments were performed on a Mettler TA Q2000 system. It was used for performing experiments for withstanding relatively high pressure to approximately 10.0 MPa. STAR^e software was applied to obtain thermal curves for further analysis (Mettler, 2004; You et al., 2010; Liu et al., 2011). Thermal decomposition characteristics of oxidation products of 1,3-butadiene were analyzed by differential scanning calorimetry (DSC). To measure the total heat, heat being evaluated during the complete cure, dynamic DSC analysis was performed from 303 to 573 K at a heating rate of 10 K·min^{-1}, and the flow of dynamic N_2 was 35.0 mL·min^{-1}. The detection sensitivity is 0.04 μW. Different masses of the three oxidation products were placed into the testing crucible. The test cell was sealed manually by a special tool equipped with Mettler's DSC.

2.5. GC-MS and HS-GC-MS analysis

The oxidation processes of 1,3-butadiene produced solid, liquid, and gaseous products. The main gas and liquid products were qualitatively analyzed by gas chromatography-mass spectrometry (GC–MS, GC/MS-QP2010 Ultra, SHIMADZU, Japan), which was performed on a GC-2010 plus gas chromatography coupled with an electron impact ionization detector (EID, 70 eV) and a Rxi-5SilMS fused silica capillary column (30 m × 0.25 mm × 0.25 μm, J&W Scientific Inc.). A sample autoinjector was employed for all liquid samples, and the gas sample was injected manually. The analytical procedures were as follows: the temperature was maintained at 333 K for 1 min, then increased to 373 K at a rate of 3 K·min^{-1}, and kept for 3 min. The carrier gas was ultrahigh pure helium at a constant flow rate of 4.0 mL·min^{-1}. The injection temperature and volume were maintained at 373 K and 1.0 μL; the split ratio was 30:1, while the interface and ion source temperatures were set at 473 and 493 K, respectively. A quadrupole mass filter was used with an m/z range of 18–300 in full-scan mode. The volatile components in the solid products were analyzed by headspace sampler-gas chromatography-mass spectrometry (HS-GC–MS) coupled with an Agilent Technologies G1888 Network Headspace Sampler. The zone temperatures were as follows: oven temperature 393 K, loop temperature 393 K, transmission line temperature 403 K. The event times were set as follows: GC cycle time 10 min, vial equilibrating time 15 min, loop fill time 0.2 min, inject time 1 min, pressurized time 0.2 min, and equilibrating loop time 0.05 min. Qualitative analysis of the products was based on the cracking patterns and retention times observed in the mass spectrometry and gas chromatography analyses, respectively.

3. Results and discussion

3.1. Pressure behavior of 1,3-butadiene oxidation in MCPVT

The oxidation of 1,3-butadiene with oxygen has been the subject of numerous publications to date, with the first report by Robey in 1944 (Robey et al., 1944). Because of its particular conjugated structure, 1,3-butadiene is readily oxidized by oxygen to generate peroxide or polyperoxide, ending in a

—O—O— bond. The peroxide is unstable and decomposes into free radicals that have a negative effect on the polymerization process. Therefore, it is vital to understand the oxidation behavior concerning oxygen and initiators in the synthesis process of styrene-butadiene rubber because their use is promoted based on their polymerization properties. The oxidation process was conducted using a self-designed MCPVT device under isothermal conditions. The MCPVT experiment was carried out under an oxygen atmosphere for three oxidation conditions: autoxidation, CHP-initiated, and AIBN-initiated. The pressure and inner temperature were monitored when the vessel was heated at 343 K for 8 h.

3.1.1. Autoxidation of 1,3-butadiene initiated by oxygen

The results of the autoxidation process and the contrast experiment in a nitrogen atmosphere are shown in Fig. 2. The temperature vs time (*T*-*t*) and pressure vs time (*P*-t) curves in Fig. 2**(b)** have no noticeable change, while the curves of Fig. 2**(a)** exhibit a significant decline. The *P*-t curve gradually declines from 0.9990 MPa to 0.9510 MPa (Table 1). It was assumed that 1,3-butadiene and oxygen are ideal gases and the two substances react in equal amounts during the reaction. Then, the amount of 1,3-butadiene remaining after the reaction was equal to the amount of oxygen, and the oxygen consumption was half of the total pressure (Table 1). The change of pressure with temperature was consistent with the ideal gas equation. Since V and R are constant values, the relationship of the amount of the total gas with time was plotted as shown in Fig. 3. Curve 1 is an approximately straight line; it indicates that a small amount of obvious chemical reactions occurred in the nitrogen atmosphere. Moreover, curve 2 for an oxygen atmosphere indicates that the reaction processes of 1,3-butadiene have occurred, with a low 1,3-butadiene conversion rate of 3.94 %.

3.1.2. Organic peroxide CHP initiated oxidation

Organic peroxide cumene hydroperoxide (CHP) has been broadly employed in the chemical industry. It is predominantly used in producing phenol and acetone by catalytic cleavage and as an initiator in the acrylonitrile–butadiene–styrene (ABS) copolymer polymerization process (Chen et al., 2008; Hsu et al., 2012; Wu et al., 2012a). CHP is easily recognized as a typical thermally unstable and hazardous substance. Therefore, this study first simulated the thermal hazard characteristics of CHP via MCPVT to predict the temperature of decomposition and the runaway behaviors. Fig. 4 demonstrates P-t and *T*-*t* curves for the decomposition of initiator CHP under the heating rate of 1.76 K·min^{-1}. The *T*-*t* curve exhibits a sharp exothermic peak. The temperature was rapidly elevated to about 408.9 K by self-decomposition when the reaction temperature reached ca. 394.65 K, accompanied by a zooming rise in pressure. It indicated that the rapid decomposition of CHP released a large amount of heat and produced two free radicals (Liu et al., 2019). The chemical entity oxidized 1,3-butadiene using the CHP as an initiator. The pressure behavior of the 1,3-butadiene oxidation process induced by 2 masses% CHP is shown in Fig. 5. The *P*-t curve displays a sharp drop and decreases from 1.0648 MPa to 0.7838 MPa (Table 1), indicating the rapid reaction of 1,3-butadiene, with a 1,3-butadiene conversion rate of 21.56 %. Also, there is a

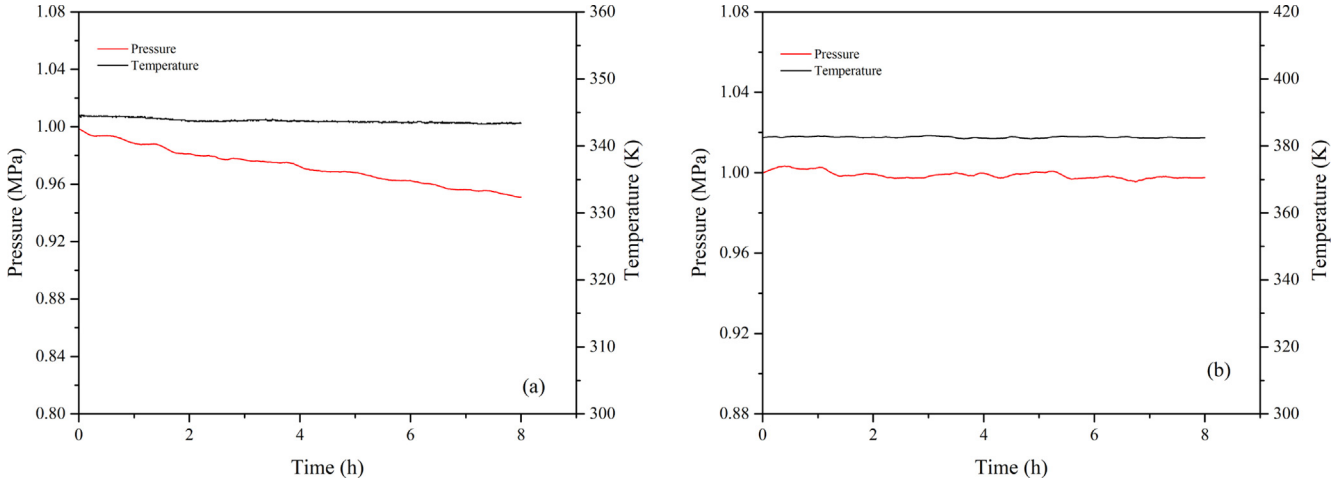

Fig. 2 The *P*-t and *T*-*t* curves of 1,3-butadiene: (a) in an oxygen atmosphere at 343 K; (b) in a nitrogen atmosphere at 383 K.

Table 1 The oxygen consumption of 1,3-butadiene oxidation.

	Autoxidation	CHP-initiated oxidation	AIBN-initiated oxidation
Initial Pressure (MPa)	0.9987	1.0445	0.9822
Final Pressure (MPa)	0.9510	0.7838	0.8824
ΔPressure (MPa)	0.0477	0.2607	0.0998
Oxygen consumption (MPa)	0.02385	0.1304	0.0499
Oxygen consumption (mmol)*	0.2406	1.3156	0.5035

* Calculated according to the ideal gas equation.

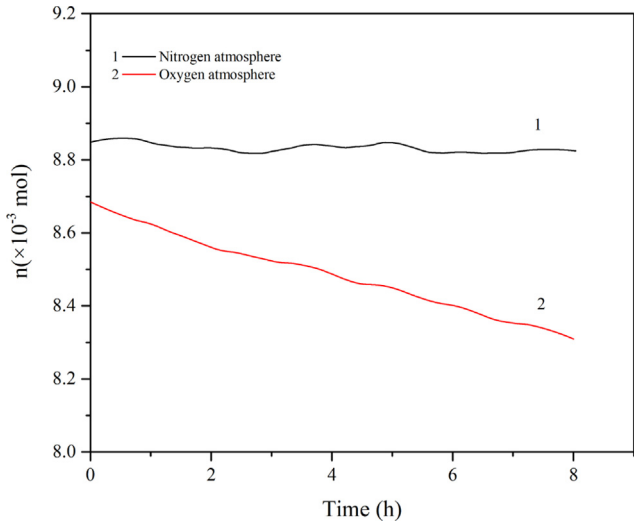

Fig. 3 The *n-t* curves of 1,3-butadiene: (1) in a nitrogen atmosphere; (2) in an oxygen atmosphere.

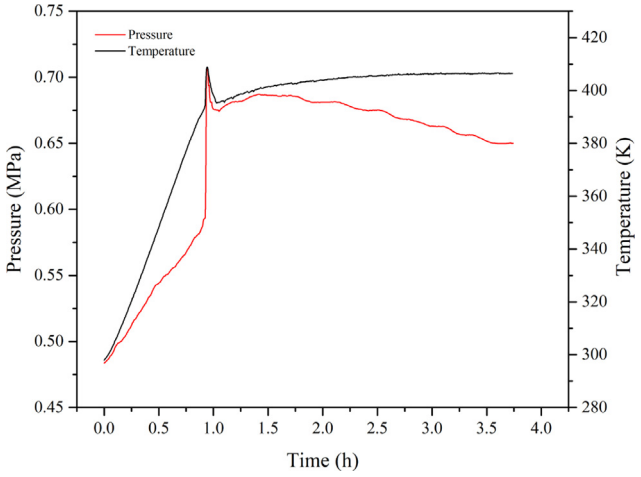

Fig. 4 The *P*-t and *T-t* curves of the CHP initiator.

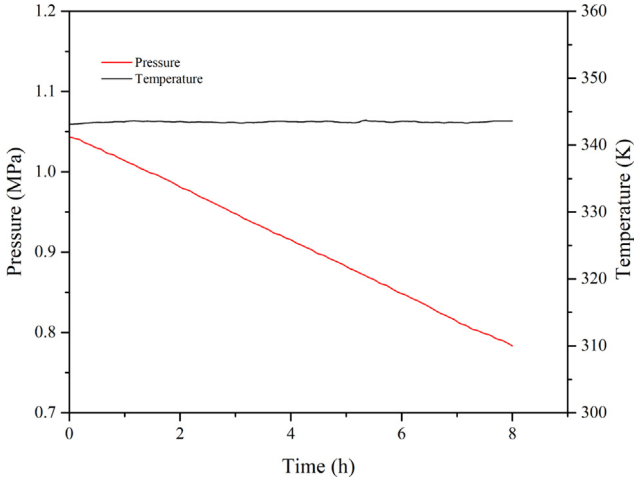

Fig. 5 The *P*-t and *T-t* curves of 1,3-butadiene initiated by CHP.

gradual visible color change of the product from colorless to yellow over time. This process is slightly different from the autoxidation approach (Table 1).

3.1.3. Azo compounds AIBN initiated oxidation

Azo compounds AIBN is a typical self-reactive material widely used for blowing agents and initiators (Guilun et al., 2013; Yamamoto and Takahashi, 2016). The pressure behavior of AIBN is shown in Fig. 6. When the oxidation temperature was raised to 342.28 K, it could be seen that there was a distinct exothermic peak on the *T-t* curves of solid AIBN during the linear heating process, causing an increase in the system temperature from 342.28 K to 381.40 K with the rate of 0.72 $K \cdot s^{-1}$. Sequentially, the system pressure increases from 0.5255 MPa to 3.6625 MPa rapidly. In that respect, the chemical nature of the AIBN initiator is the free radical formed following the thermal initiation reaction.

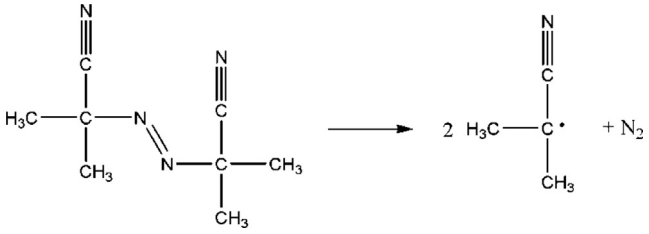

The oxidation of 1,3-butadiene initiated by AIBN was also investigated. According to Fig. 7, time course studies of MCPVT analysis have shown a quick decline of the pressure, with the value decreasing from 0.9899 MPa to 0.8824 MPa (Table 1), which indicates a chemical reaction occurred between reactants. Similarly, this process was accompanied by a gradual visible color change of the product from colorless to brown over time. These oxidized products were identified based on GC–MS and HS-GC–MS analyses in this work below.

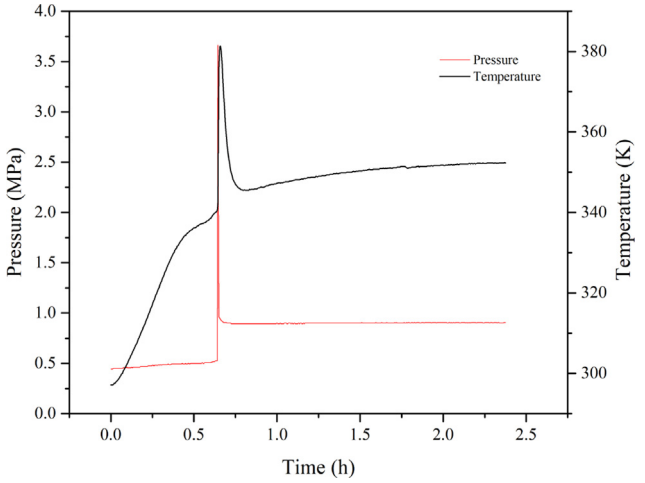

Fig. 6 The *P*-t and *T-t* curves of the AIBN initiator.

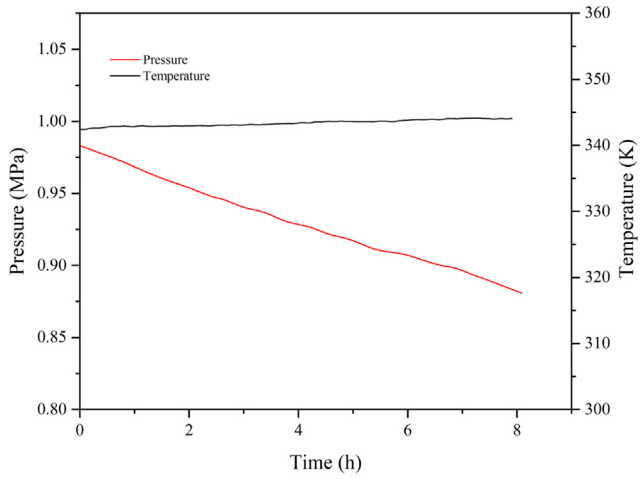

Fig. 7 The *P*-t and *T*-*t* curves of 1,3-butadiene initiated by AIBN.

3.2. Oxidation kinetic

The oxidation reaction of 1,3-butadiene was affected by the presence of oxygen and initiator and further affected its thermal stability. In order to control the oxidation reaction process, the influence of reaction conditions (temperature and initiator) on the oxidation reaction rate of 1,3-butadiene was studied. The initiators and the peroxides products would decompose into many free radicals during its deep radical oxidation process. Those free radicals would lead to the reaction of 1,3-butadiene being complicated. Thus, this paper only discussed the kinetics of the initial oxidation reaction of 1,3-butadiene. To determine the initial oxidation rate of 1,3-butadiene under oxygen and initiator, two kinetic models, viz. autoxidation and initiated oxidation, were applied. In an autoxidation model, 1,3-butadiene reacted with oxygen and gave rise to polyperoxide, which was unstable and decomposed into a mass of free radicals. It would initiate the dimerization of 1,3-butadiene. Dimerization of 1,3-butadiene through the Diels-Alder reaction is second-order in the gas phase (Aldeeb et al., 2004). Based on that, the autoxidation model was expressed as the following equation:

$$B + O_2 \rightarrow \text{Products} \quad R_o = -\frac{d[B]}{dt} = k_o[B][O_2] \tag{3}$$

$$B + B \rightarrow \text{Products} \quad R_d = -\frac{d[B]}{dt} = k_d[B]^2 \tag{4}$$

where k_0 and k_d are the apparent rates constant of oxidation and dimerization, $mol^{-1}\cdot h^{-1}$, respectively; t is the reaction time, h; $[B]$ and $[O_2]$ are the concentrations of 1,3-butadiene and oxygen at time t, respectively, $mol\cdot L^{-1}$.

To simplify the equation, the C_4H_6:O_2 ratio in the experiment was near unity. The alternating (1 to 1) copolymer of 1,3-butadiene and oxygen was mainly formed in the oxygen atmosphere (Hendry et al., 1968a,b). Under this condition, the same amount of 1,3-butadiene and oxygen was consumed in the oxidation reaction. That was, $[B] = [O_2]$. Since the two reactions occurred almost simultaneously, these could be treated as parallel reactions (Ren et al., 2015) Then, the total rate equation for Eqs. (3) and (4) is:

$$R_{b1} = -\frac{d[B]}{dt} = k_1[B]^2,\ k_1 = k_o + k_d \tag{5}$$

In addition, the oxidation and dimerization reactions mainly form liquid or solid products, and the vapor pressure of gas products can be negligible. It was assumed that both 1,3-butadiene and oxygen are ideal gases; an ideal gas state equation was employed to quantify the number of reactants.

$$R_{b1} = -\frac{d[P]}{dt} = k_P[P]^2,\ k_P = k_1\frac{V}{RT} \tag{6}$$

where P is the pressure at time t, k_P is the total rate constant, $MPa^{-1}\cdot h^{-1}$, V is a constant, 25 mL; R is the universal constant (8.314 $J\cdot mol^{-1}\cdot K^{-1}$). Therefore, Eq. (6) can be transferred as:

$$\frac{1}{P} = k_P t + C \tag{7}$$

where C is a constant.

Meanwhile, the mechanism for the oxidation of 1,3-butadiene under the initiator was shown as follows (Mayo et al., 1957; Mayo, 1958; Hendry et al., 1968a,b). Where B is a 1,3-butadiene molecule, B·, and BO_2· are radicals of 1,3-butadiene and oxygen units, and In· is a radical from the initiator.

Initiation reactions

$$\text{Initiator} \xrightarrow{k_i} 2In\cdot \quad R_i = 2k_i[In\cdot] \tag{8}$$

$$In\cdot + O_2 \xrightarrow{k_{io}} InO_2\cdot \quad R_{io} = k_{io}[In\cdot] \tag{9}$$

Propagation reactions

$$InO_2\cdot + B \xrightarrow{k_{ob}} B\cdot \tag{10}$$

$$B\cdot + O_2 \xrightarrow{k_{bo}} BO_2\cdot \quad R_{bo} = k_{bo}[B\cdot][O_2] \tag{11}$$

$$BO_2\cdot + B \xrightarrow{k_{bob}} B\cdot \tag{12}$$

$$B\cdot + B \xrightarrow{k_{bb}} BO_2\cdot \quad R_b = k_{bob}[BO_2\cdot][B] + k_{bb}[B\cdot][B] \tag{13}$$

Termination reactions

$$2BO_2\cdot \xrightarrow{k_{io}} \tag{14}$$

$$BO_2\cdot + B\cdot \xrightarrow{k_{iob}} \text{nonradical products} \tag{15}$$

$$2B\cdot \xrightarrow{k_{ib}} \tag{16}$$

For long kinetic chains at high oxygen pressures (where reactions (13), 15, and 16 can be neglected), the conventional steady-state assumption gives

$$R_{b2} = \left(\frac{R_i}{2k_{io}}\right)^{\frac{1}{2}} k_{ob}[B] \tag{17}$$

Then

$$R_{b2} = -\frac{d[B]}{dt} = k_2[B],\ k_2 = \left(\frac{R_i}{2k_{io}}\right)^{\frac{1}{2}} k_{ob} \tag{18}$$

Assuming that 1,3-butadiene is an ideal gas, the concentration of 1,3-butadiene can be approximated by the ideal gas equation ($PV = nRT$). Eq. (18) can be rearranged as

$$R_{b2} = -\frac{dP}{dt} = k_2 P \tag{19}$$

Then.

$$\ln P = -k_2 t + C \quad (20)$$

The activation energy E_a and frequency factor A were determined by plotting the experimental rate constants obtained at different temperatures from the linear form of the Arrhenius equation (Eq. (21)).

$$\ln k = -\frac{E_a}{RT} + \ln A \quad (21)$$

From Eq. (21), the value of activation energy can be determined based on the slope, and the intercept can obtain the frequency factor.

For the experiment, the initial temperatures of the 1,3-butadiene oxidation process were 323 K, 333 K, 343 K, 353 K, and 363 K. The kinetic calculations began with the decrease of pressure, which was recorded as 0 h. Fig. 8 shows the plots of $1/P$ vs time t at different temperatures for the autoxidation model. Fig. 9 displays the curves of ln P vs time t at different temperatures for two initiated oxidation models. The kinetic parameters are displayed in Table 2. It indicated the reaction rates had different degrees of increasing with an increasing temperature. The initial reaction rate of autoxidation increased lightly with the increasing temperature, while the reaction rates of CHP and AIBN-initiated oxidation were remarkably improved. Adding initiators could be accelerated the oxidation to form more peroxides, which would be attributed to the formation of free radicals through decomposition (Wang et al., 2018). Furthermore, the reaction rate initiated by CHP was greater than that of AIBN-initiated. Such a trend suggests that organic peroxide compound has more effect than azo compound in enhancing the reactivity of 1,3-butadiene toward oxygen.

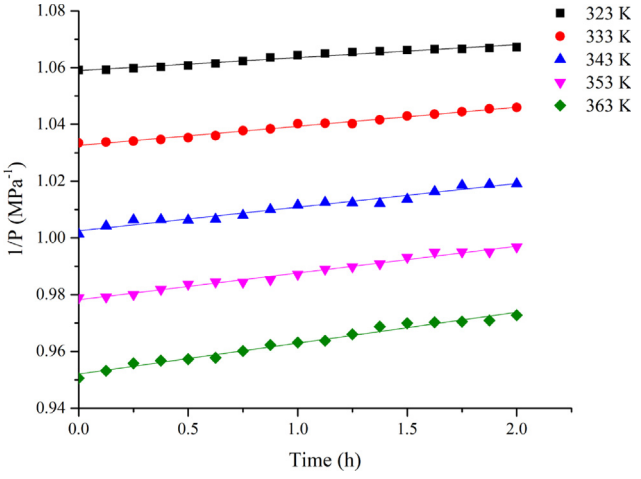

Fig. 8 Plot of $1/P$ vs t for 1,3-butadiene autoxidation model.

The activation energies were calculated by the Arrhenius equation (Eq. (21)), and plots of ln k vs T^{-1} consisted of straight lines (Fig. 10). The slope to calculate the activation energy is displayed in Table 3. Autoxidation's apparent activation energy (E_a) was calculated to be 20.85 kJ·mol^{-1}. In two initiated oxidation models, the apparent activation energies E_a were 33.30 kJ·mol^{-1} and 56.27 kJ·mol^{-1}, respectively, which were more extensive than autoxidation. There were two reasons for these differences. First, the autoxidation of 1,3-butadiene followed second-order reaction kinetics, whereas the initiated oxidation models were fitted to first-order reactions. Those corresponded to different reaction mechanisms, autoxidation, and free radical initiated mechanisms. Second, the initial onset temperature T_0 of 80 mass% CHP and pure AIBN were calculated to be 373 K and 383 K, respectively (Wu et al., 2012b; Zhang et al., 2015). *Activation energy* is the minimum energy required to initiate a reaction, which implies that a reaction with higher activation energy either needs a higher reaction temperature to gain adequate energy to initiate the reaction (Vuppaladadiyam et al., 2019). Therefore, the E_a of CHP-initiated oxidation was lower than that of AIBN-initiated oxidation. It indicated that the oxidation rates of different reaction systems and activation energy varied significantly. Hendry et al. (1968a,b) studied that the rate of the liquid-phase oxidation of 1,3-butadiene initiated by AIBN was 0.036 Mole·h^{-1} at 760 Torr oxygen at 50 ℃ for 7.57 h. Aldeeb et al (Aldeeb et al., 2004) reported the reaction of 1,3-butadiene with oxygen fit with second-order, and the activation energy was 20.1 ± 2.1 kcal·mol^{-1}. Adusei et al (Adusei and Fontijn, 1993) researched the rate coefficients for consumption of ground-state oxygen atoms by reaction with 1,3-butadiene in the temperature range of 324 K to 363 K have

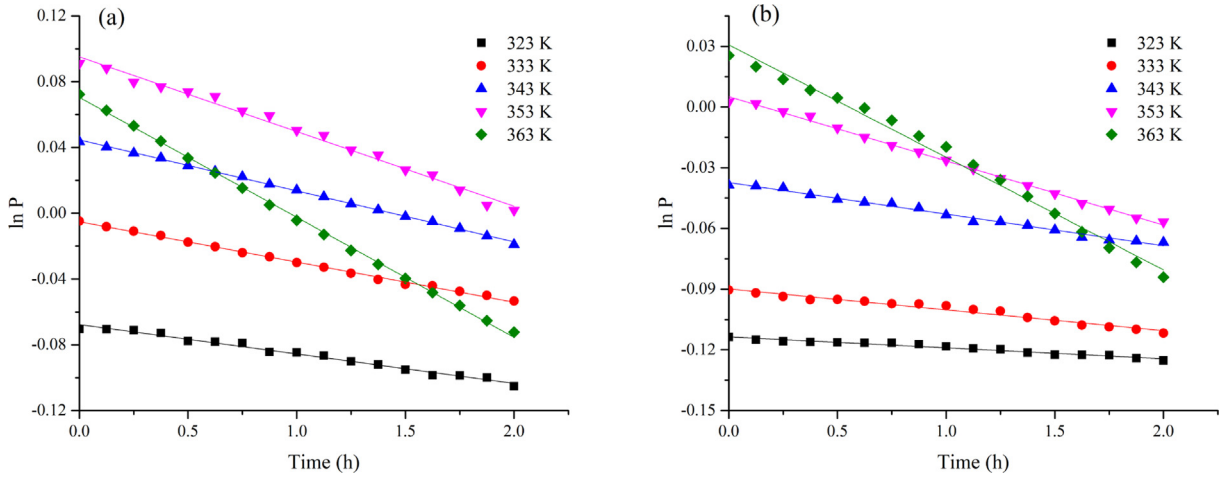

Fig. 9 Curves for initiated oxidation models of 1,3-butadiene; (a) CHP-initiated oxidation; (b) AIBN-initiated oxidation.

Table 2 Kinetics parameters for three oxidation models of 1,3-butadiene at different temperatures.

T(K)	Autoxidation		CHP-initiated oxidation		AIBN-initiated oxidation	
	$k \times 10^{-2}$ (MPa^{-1}·h^{-1})	R^2	$k \times 10^{-2}$ (MPa·h^{-1})	R^2	$k \times 10^{-2}$ (MPa·h^{-1})	R^2
323	0.4578	0.9627	1.790	0.9859	0.5421	0.9654
333	0.6694	0.9869	2.442	0.9977	1.031	0.9691
343	0.8346	0.9637	3.101	0.9989	1.561	0.9887
353	0.9454	0.9868	4.544	0.9901	3.175	0.9973
363	1.086	0.9798	7.298	0.9991	5.560	0.9907

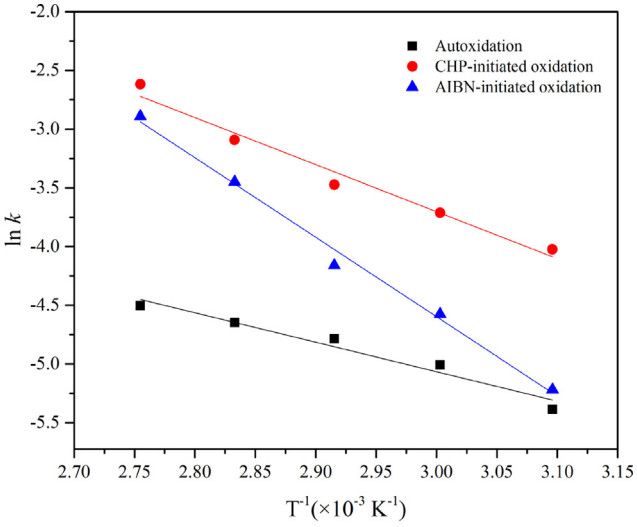

Fig. 10 Plots of ln k vs T^{-1}.

been measured. The results revealed that the average rate coefficient and the activation energy were 1.74×10^{-11} cm^3·mol^{-1}·s^{-1} and 27.42 kJ·mol^{-1}, respectively. Liu et al (Liu et al., 1988) investigated that the absolute rate constants for the gas-phase reaction of the OH radical with 1,3-butadiene in an argon atmosphere were measured at 1 atm over the temperature range 305–1173 K. At temperatures below 600 K, k(OH + 1,3-butadiene) = $(1.4 \pm 0.1) \times 10^{-11}$ exp[(440 ± 40)/T]cm^3·mol^{-1}·s^{-1}. The thermal polymerization and oxidation characteristics of 1,3-butadiene were investigated using an ARC by Liu et al (Liu et al., 2020). The result showed that the activation energy of 1,3-butadiene oxidation was 112.6 kJ·mol^{-1}.

3.3. Peroxide value of 1,3-butadiene peroxide

In the presence of oxygen, 1,3-butadiene reacts with oxygen and possibly results in the formation of peroxide. In order to further confirm this result, the peroxide values of three kinds of oxidation processes were analyzed by iodimetry. The iodimetry results showed that 1,3-butadiene would produce different peroxide content under different oxidation processes. The effect of the main reaction conditions (reaction time, temperature, the molar ratio of 1,3-butadiene-to-oxygen, and initiators) on the peroxide value of the oxidation reaction was investigated, with the results shown in Fig. 11. The influence of reaction time on peroxide value is shown in Fig. 11**(a)**. The relationship between the peroxide value and the oxidation reaction time is as follows: when the reaction time was from 0 h to 20 h, the peroxide value increased slowly from 0 to 2.37 mmol·kg^{-1}; when the reaction time was from 20 h to 26 h, the peroxide value increased rapidly from 2.37 mmol·kg^{-1} to 27.76 mmol·kg^{-1}; at t = 26 h, the maximum peroxide value is obtained; when the reaction time was from 26 h to 30 h, the peroxide value decreased quickly from 27.76 mmol·kg^{-1} to 8.5 mmol·kg^{-1}.

The initial reaction of 1,3-butadiene with oxygen is to produce peroxide, but peroxide is unstable and prone to thermal decomposition reaction. That is, the oxidation reaction of 1,3-butadiene with oxygen is:

$$\text{Oxidation: 1,3-butadiene} + O_2 \rightarrow \text{Peroxides} \quad (22)$$

$$\text{Decomposition: Peroxides} \rightarrow \text{Free radical} \quad (23)$$

$$\text{Complex reaction: Peroxides (or 1,3-butadiene)} + \text{Free radical} \rightarrow \text{Complex products} \quad (24)$$

From the above reactions, it can be seen that in the initial reaction (22) stage, the reaction is dominated by the formation of peroxide, and the peroxide concentration increases with time. Due to the interaction of Eq. (22) and (23), the peroxide concentration will reach the maximum of 27.76 mmol·kg^{-1} (at 26 h and 338 K). Free radicals are very active and can trigger many reactions, including autocatalytic reactions. At a specific temperature (e.g. 338 K), the peroxide concentration cannot maintain a stable maximum value because Eq. (24) decreases with time. In order to reduce the thermal decomposition of peroxide, it is possible to reduce the reaction temperature.

The effect of temperature on peroxide value is shown in Fig. 11**(b)**. The concentration first increased from 3 mmol·kg^{-1} to 27.85 mmol·kg^{-1} with increasing temperature from 318 K to 338 K at 26 h, indicating more and more peroxides were produced. Then it decreased with increasing temperature after 338 K. Peroxides are temperature-dependent and decompose at high temperatures. Handy and Rothrock have reported that the primary product from the oxidation of 1,3-butadiene at 353 K is a nonvolatile copolymer of 1,3-butadiene and oxygen, which contained 1,2- and 1,4-butadiene units as polybutadiene, but some or all of these units are separated by peroxide (—O—O—) links (Handy and Rothrock, 1958). The unstable —O—O— bond of peroxide was prone to decompose under high temperatures and would give rise to many free radicals that promote the deep oxidation of 1,3-butadiene with oxygen. The free radical was conducted in combination with those MCPVT observation results.

The effect of the molar ratio of 1,3-butadiene-to-oxygen on peroxide value was assessed. Fig. 11**(c)** shows that the peroxide value increased with an increasing molar ratio, indicating that

Table 3 The activation energy for three oxidation models.

Oxidation model	Reaction order	Equation	E_a (kJ·mol^{-1})	R^2
Autoxidation	2nd order	$\ln k = -2508.2 \times T^{-1} + 2.459$	20.85	0.9615
CHP-initiated oxidation	1st order	$\ln k = -4005.1 \times T^{-1} + 8.313$	33.30	0.9749
AIBN-initiated oxidation	1st order	$\ln k = -6768.7 \times T^{-1} + 15.71$	56.27	0.9930

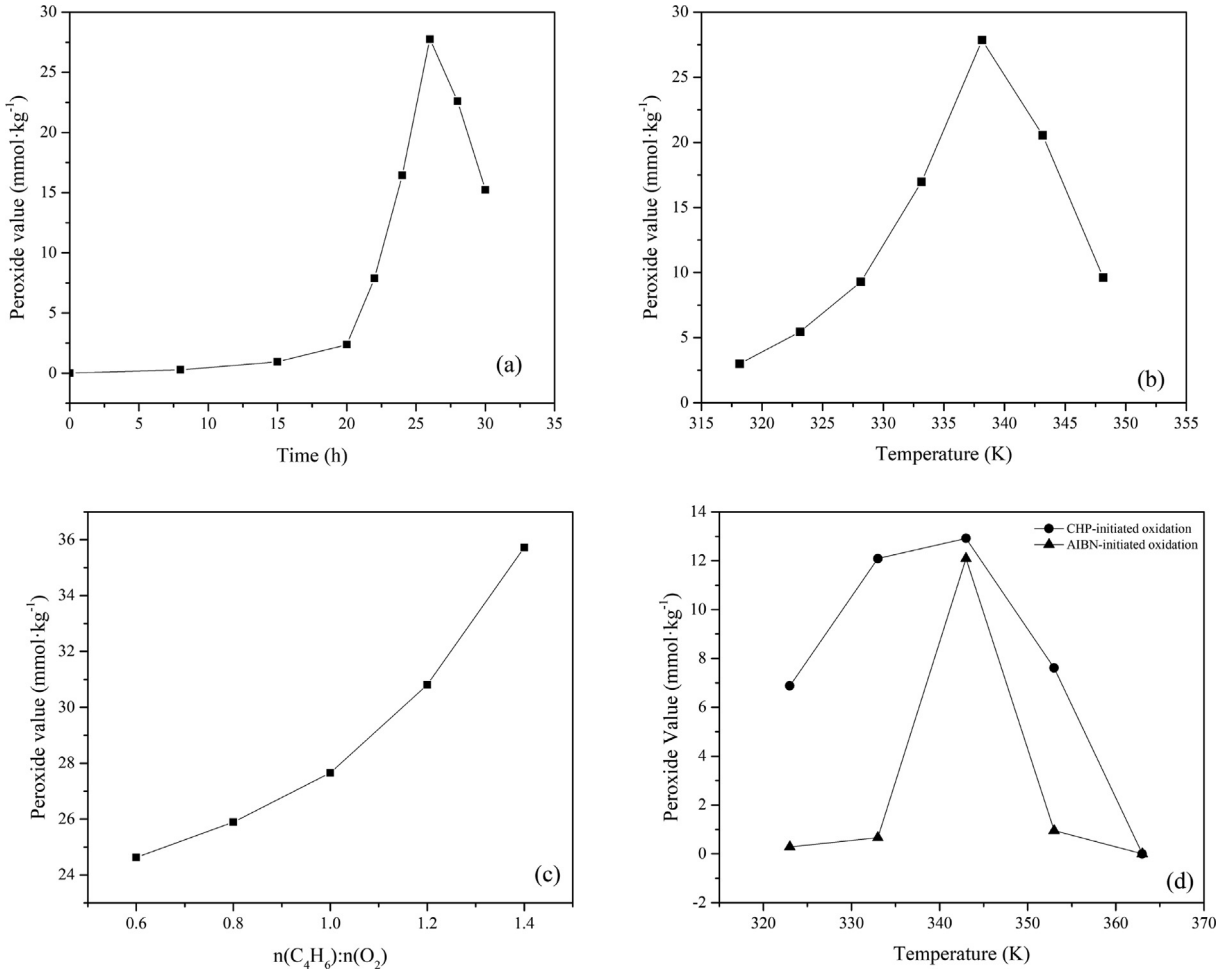

Fig. 11 Effects of the reaction conditions on the peroxide value of autoxidation reaction. (a) Reaction time; (b) Reaction temperature; (c) The C_4H_6: O_2 molar ratio; (d) Initiated oxidation.

1,3-butadiene reacted completely with oxygen and produced more peroxides. The effect of initiators on peroxide value was discussed in Fig. 11**(d)**. As proposed in Section 3.2, the reaction rate of the 1,3-butadiene oxidation process increased in the initiators' presence. So, the reaction time of 1,3-butadiene oxidation initiated by initiators was reduced to 8 h to detect the peroxide value. The results showed that the CHP-initiated oxidation would form a high level of peroxide during its oxidation process at 343 K, reaching the highest value of 12.92 mmol·kg^{-1}, then decreased with the reaction temperature increased. The peroxide value of AIBN-initiated reached the highest value of 12.09 mmol·kg^{-1}, which was less than that of CHP-initiated. Thus, it is notable that 1,3-butadiene had a vital ability for peroxide production in contact with oxygen and tended to proceed with the decomposition of peroxide to form oxidation products.

3.4. Thermal decomposition characteristics of oxidation products

DSC is a standard instrument used to measure organic matter's oxidation stability and organic peroxide's decomposition heat (Chen et al., 2008; Zhang et al., 2015). Li et al. reported that peroxide was an important energetic material with potential hazards because its decomposition releases heat (Li et al., 2019). In order to investigate the relationship between peroxide value and heat release, peroxides with different peroxide values were measured by DSC. The exothermic onset temperature

(T_0) and the heat of decomposition (Q_{DSC}) of peroxide were measured by the thermal curves of the DSC by dynamic thermal scanning under a heating rate of 10 K·min^{-1}.

Different peroxide values were measured to analyze exothermic reactions, as shown in Fig. 12. It can be seen that there are distinct exothermic peaks on the DSC curves of 1,3-butadiene oxidation products. The results show that the peroxide value increased from 15.3 mmol·kg^{-1} to 33.6 mmol·kg^{-1}, corresponding to the decomposition heat Q_{DSC} increased from 897.2 J·g^{-1} to 1887 J·g^{-1} (Table 4). According to the United Nations Publication Recommendations on the Transport of Dangerous Goods (Persson et al., 2018), the substance could be classified as the fifth type of hazardous material because its Q_{DSC} exceeds 250.0 J·g^{-1}. It indicated that the oxidation products were hazardous. Besides, the T_0 was determined to be advanced and decreased with the increase of peroxide value. It indicated that a higher starting temperature would inevitably cause significant runaway behavior to appear earlier, resulting in the safety of production, transportation, and usage being threatened.

DSC also measured the oxidation products of 1,3-butadiene initiated by initiators, and the results are shown in Fig. 13. The heat flow curves of CHP and AIBN-initiated products performed strongly exothermic peaks at the temperature range of 334.62–453.84 K, and its decomposition heat was 826.6 J·g^{-1} and 1152.8 J·g^{-1}, respectively. However, these peak patterns showed a significant difference from autoxidation, which residual initiators in the oxidation products may cause. In the previous work, to prevent the thermal explosion of 80 mass% CHP for transportation, manufacturing process, or use, Wu et al. analyze thermal hazards and safe storage of 80 mass% CHP (Wu, 2012). The T_0 of 80 mass% CHP by DSC was calculated to be 373 K, and the Q_{DSC} was determined to be 1200 J g^{-1} with a heating rate of 10 K·min^{-1}. In addition, the thermal decomposition characteristic of AIBN was investigated by Zhang et al (Zhang et al., 2015). The T_0 of AIBN by DSC was calculated to be 383 K, and the Q_{DSC} was determined to be 1024 J g^{-1} with a heating rate of 10 K·min^{-1}. Therefore, the exothermic peak was widened, and the T_0 was advanced in the presence of the initiator. The thermal parameters of three kinds of products are shown in Table 4. The

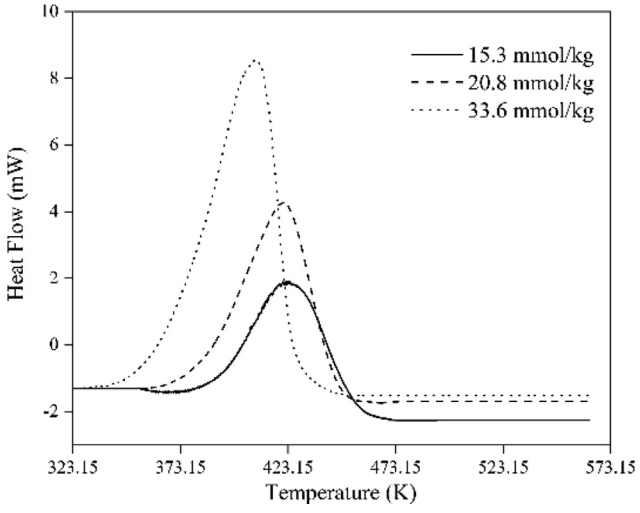

Fig. 12 Heat flow vs temperature for autoxidation products.

decomposition of peroxide can cause potential thermal hazards and release radicals to form many secondary products.

3.5. Products of 1,3-butadiene oxidation

To further characterize the complicated 1,3-butadiene oxidized products, the oxidized products were collected and monitored by GC-MS and HS-GC–MS. The relative quantities of each identified component were estimated based on the peak area. The gas products are shown in Table 5. Similar oxidized products were produced from three oxidation models for autoxidation, CHP-initiated oxidation, and AIBN-initiated oxidation of 1,3-butadiene. Furan is the main gas product, with a low 1,3-butadiene conversion rate of 0.19 %, 0.87 %, and 0.21 %, respectively. In the case of CHP-initiated oxidation, additional products of 2-propenal and formic acid were formed with a relative content of 0.30 % and 1.65 %, respectively.

The liquid products are summarized in Table 6. In the case of autoxidation, the six main products were 1,2-divinlcyclobutane, 3-butene-1,2-diol, 2(5H)-furanone, 4-vinylcyclohexene, allyl alcohol and 2,6-cyclooctadien-1-one with relative contents of 0.75 %, 0.64 %, 3.63 %, 25.38 % 1.33 %, and 0.58 %, respectively. The main dimerization products were 1,2-divinlcyclobutane and 4-vinylcyclohexene, whereas the other four were oxidation products. It can be inferred that autoxidation of 1,3-butadiene was undergone with a low conversion rate. As a comparison, the products of CHP and AIBN-initiated oxidation were also determined. Many aldehydes, acids, and alcohols were produced with a high 1,3-butadiene conversion rate. In the case of AIBN-initiated oxidation, 4-vinylcyclohexene (28.67 %) was still the major product, but the yield of oxidized products had increased to 23.30 %. It indicated AIBN initiator promoted the oxidation of 1,3-butadiene. Besides, the quantities of the main products resulting from CHP-initiated oxidation were 2-propenal, allyl alcohol, and 3-cyclohexene-1-carboxylic acid, with relative content of 10.08 %, 15.96 %, and 8.22 %, respectively. Compared to autoxidation, the yields of similar oxidized products for 3-butene-1,2-diol, 2(5H)-furanone, allyl alcohol, and 2,6-cyclooctadien-1-one were increased. It indicated that the CHP initiator significantly affects the oxidation of 1,3-butadiene. Table 7 displays the volatile components in solid products of 1,3-butadiene oxidation. The main products were 2(5H)-furanone and 4-vinylcyclohexene. Therefore, results from the GC-MS and HS-GC-MS indicated that each oxidation mode produced a more or less similar set of oxidized products. For two initiated oxidation models, CHP and AIBN are initiators of free radical chain reactions, but the initial decomposition temperatures were different. The oxidation of 1,3-butadiene was initiated by the free radicals generated from the initiators. At the same temperature and time, the degrees of 1,3-butadiene oxidation initiated by various initiators were different, which led to different results for the measured product distribution. For the autoxidation model, there are two steps: the reaction of 1,3-butadiene with oxygen was dominated by the formation of peroxides, and peroxides would further decompose to initiate the complex reaction. The initial oxidation reaction could also lead to the different distribution of 1,3-butadiene reaction products.

Table 4 Thermal parameters for the products of three oxidation models by DSC at 10 K·min^{-1}.

Oxidation model	Mass (mg)	Peroxide value (mmol·kg^{-1})	T (K)	T_0 (K)	T_{offset} (K)	T_p (K)	Q_{DSC}(J·g^{-1})
Autoxidation	0.99	15.3	374.15–473.91	391.55	448.41	423.99	897.2
	1.12	30.8	358.15–457.95	381.75	438.49	420.86	1184
	1.22	33.6	335.15–452.03	367.52	419.32	407.29	1887
CHP-initiated oxidation	1.68	12.92	343.53–453.83	346.13	445.03	412.85	828.6
AIBN-initiated oxidation	1.56	12.09	334.62–453.84	355.40	440.15	399.08	1152.8

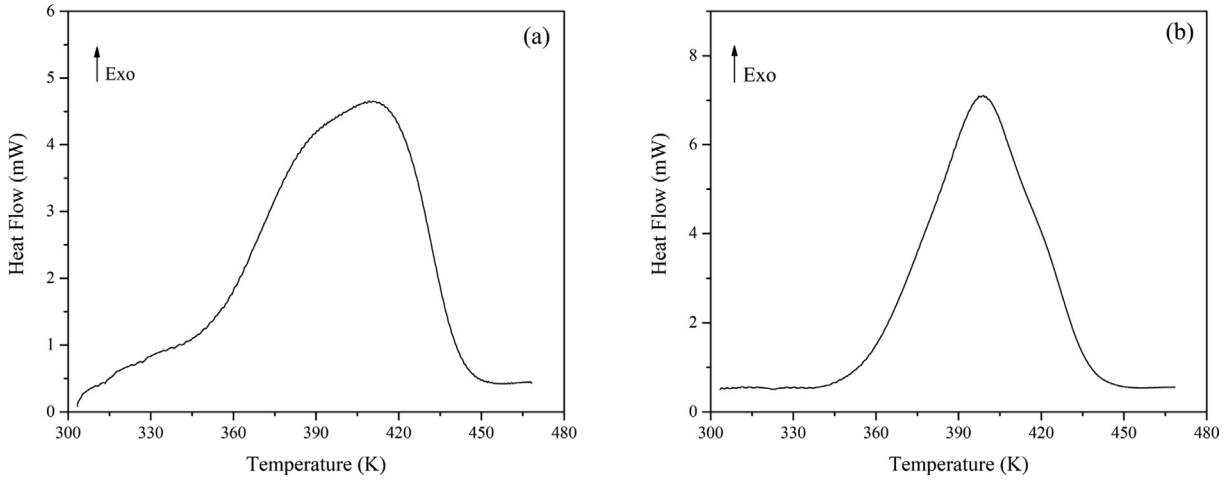

Fig. 13 Heat flow vs temperature for initiated oxidation products. (a) CHP-initiated oxidation; (b) AIBN-initiated oxidation.

Table 5 Identified gas products of 1,3-butadiene for three oxidation models.

NO.	Components	Molecular formula	Relative content %			Similarity %
			Autoxidation	CHP-initiated oxidation	AIBN-initiated oxidation	
1	Oxygen	O_2	47.39	46.74	43.00	91
2	Water	H_2O	2.95	2.73	3.35	100
3	1,3-Butadiene	C_4H_6	49.47	47.70	53.43	96
4	2-Propenal	C_3H_4O		0.30		92
5	Furan	C_4H_4O	0.19	0.87	0.21	95
6	Formic acid	$C_3H_6O_2$		1.65		98

There are two reactions of 1,3-butadiene in an oxygen atmosphere: (1) oxidation reaction; (2) polymerization. Under a nitrogen atmosphere, the reaction products of 1,3-butadiene are not detected even if the temperature is 373 K. When the temperature is 383 K, a small amount of chemical reaction occurs. The main products are 1,3-butadiene dimers, including 4-vinylcyclohexane and 1,2-divinylcyclobutane. However, the 1,3-butadiene oxidation reaction can quickly occur in an oxygen atmosphere. When the temperature is 343 K, there are many reaction products, including oxidation products (oxygenated compounds) and polymers (such as dimers). The results show that the autoxidation reaction can significantly reduce the reaction temperature of 1,3-butadiene.

A possible scheme of 1,3-butadiene oxidation is proposed, as shown in Scheme 1. There are two possible pathways. The first pathway is the oxidation process of 1,3-butadiene. As a result of O-atom addition to the π bond in 1,3-butadiene, two possible biradical isomers could be produced after the initiator and O_2 addition. The isomerization of 1,4-buteneperoxy radical (isomer **A**) would lead to the formation of 3,6-dihydro-1,2-dioxin (DHD), a highly reactive peroxide that may initiate the polymerization of the 1,3-butadiene (Aldeeb et al., 2004). This peroxide was instability and formed 2,5-dihydrofuran. It is known that 2,5-dihydrofuran undergoes H_2 elimination to produce furan (Assa et al., 1986; Wellington and Walters, 2012). The other isomer, 1,2-buteneperoxy radical (isomer **B**), was favorable to isomerizing vinyloxirane, which underwent rapid ring expansion to 2,3-dihydrofuran at relatively low temperatures (Crawford et al., 1976) The reactions of 2,3-dihydrofuran were reported (Assa and Menashe, 1989) as unimolecular isomerization to crotonaldehyde and cyclopropanecarboxaldeldehyde. The formation of crotonaldehyde can be inferred based on previous work (Lifshitz and Laskin, 1994) on the thermal reactions of 2-methyl-4,5-

Table 6 Identified liquid products of 1,3-butadiene for three oxidation models.

NO.	Components	Molecular formula	Relative content %			Similarity %
			Autoxidation	CHP-initiated oxidation	AIBN-initiated oxidation	
1	Water	H_2O	1.04	0.53	0.55	81
2	1,3-Butadiene	C_4H_6	65.52	36.98	39.45	90
3	2-Propenal	C_3H_4O		10.08	8.01	93
4	3,4-Dihydro-2H-pyran	C_5H_8O		5.30	3.07	85
5	Acetone cyanohydrin	C_4H_7NO			2.14	80
6	1,2-Divinlcyclobutane	C_8H_{12}	0.75			85
7	Propanal	C_3H_6O		0.24	0.10	84
8	Cyclopropanecarboxylic acid	C_4H6O_2		2.63	0.76	85
9	3-Butene-1,2-diol	$C_4H_8O_2$	0.64	3.49	1.86	91
10	4-Vinylcyclohexene	C_8H_{12}	25.38	5.30	28.67	97
11	Allyl formate	$C_4H_6O_2$		0.67		82
12	2(5H)-Furanone	$C_4H_4O_2$	3.63	1.19	0.35	91
13	Cumene	C_9H_{12}		1.34		94
14	Propionic anhydride	$C_6H_{10}O_3$		0.05	0.33	88
15	Allyl alcohol	C_3H_6O	1.33	15.96	5.80	89
16	2-Butene-1,4-diol	$C_4H_8O_2$		0.72	0.50	86
17	9-Oxabicyclo[6.1.0]non-4-ene	$C_8H_{12}O$			1.66	82
18	2,2′-Azobisisobutyronitrile (AIBN)	$C_8H_{12}N_2$			0.81	93
19	2,6-Cyclooctadien-1-ol	$C_8H_{12}O$			0.37	83
20	Acetophenone	C_8H_8O		0.81		96
21	2,6-Cyclooctadien-1-one	$C_8H_{10}O$	0.58	3.11	3.23	87
22	2-Phenyl-2-propanol	$C_9H_{12}O$		0.48		93
23	5,10-Dioxatricyclo[7.1.0.0^{4,6}] decane	$C_8H_{12}O_2$			0.53	86
24	3-Cyclohexene-1-carboxylic acid	$C_7H_{10}O_2$		8.22	0.40	83
25	3-Cyclohexene-1-carboxaldehyde	$C_7H_{10}O$		2.25	0.60	82
26	Unknown component		1.13	0.68	0.80	

Table 7 Identified volatile components in solid products of 1,3-butadiene for three oxidation models.

NO.	Components	Molecular formula	Relative content %			Similarity %
			Autoxidation	CHP-initiated oxidation	AIBN-initiated oxidation	
1	2(5H)-Furanone	C_4H_4O	35.12	34.34	58.23	82
2	1,2-Divinylcyclobutane	C_8H_{12}	1.67			91
3	4-Vinylcyclohexene	C_8H_{12}	63.21	18.18	36.71	93
4	3-Cyclohexene-1-carboxaldehyde	$C_7H_{10}O$		5.05		90
5	α-Methylstyrene	C_9H_{10}		27.27		94
6	2,2′-Azobisisobutyronitrile	$C_8H_{12}N_2$			5.06	86
7	Acetophenone	C_8H_8O		15.15		94

dihydrofuran, which showed that 2,3-dihydrofuran could isomerize either directly to a noncyclic aldehyde or via the cyclopropane to form the noncyclic aldehyde. Besides, at one-atmosphere pressure, collisions would be instrumental in the biradical isomer **B** undergoing a 1,2-hydrogen shift to form 3-butenal (Brezinsky et al., 1985). It was expected to react in a way characteristic of aldehydes (Colket et al., 1977). In the presence of abundant OH, H, and O, the easily abstractable aldehyde H is removed and is followed by the loss of CO. In this case, the resonantly-stabilized long-lived allyl radical is formed and is postulated to react with either O or HO_2 in a radical–radical reaction to form acrolein (Brezinsky et al., 1985). The two biradical isomers could form 2-butene-1,4-diol and 3-butene-1,2-diol via H-addition (Handy and Rothrock, 1958; Zhang et al., 2019). The deep radical oxidation of 1,3-butadiene is a remarkably complex reaction. The reaction of 1,3-butadiene with oxygen could give rise to an unstable peroxide. The spontaneous homolysis of the —O—O—

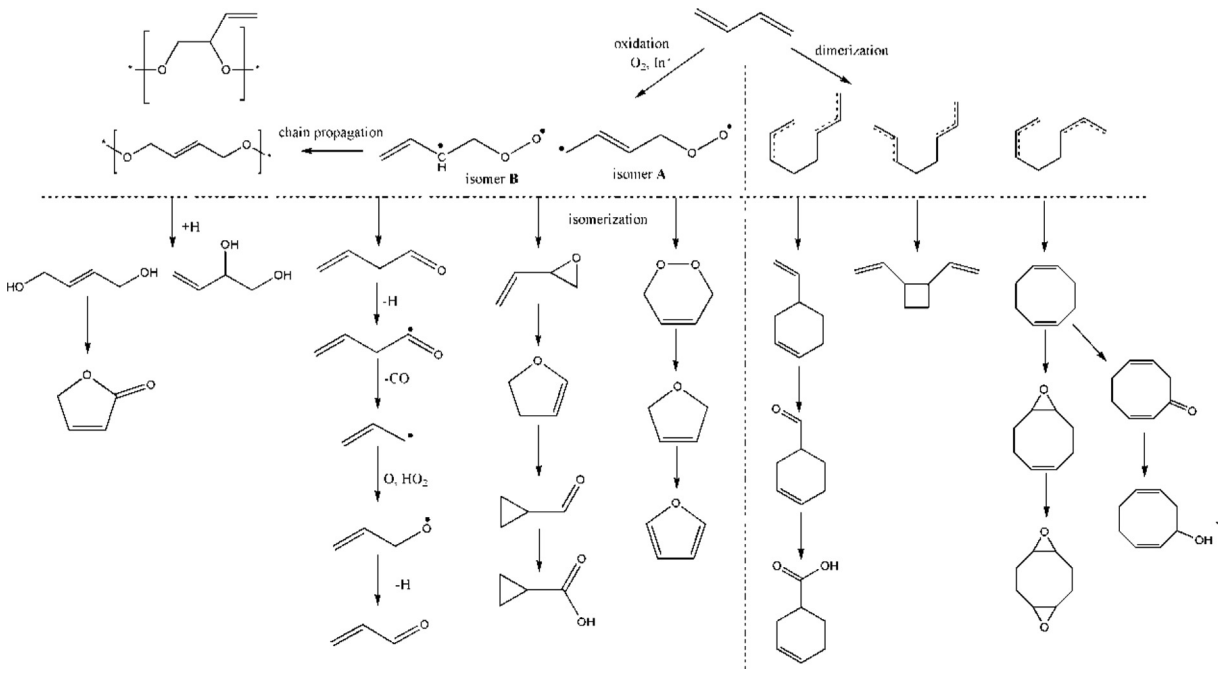

Scheme 1 The possible scheme of 1,3-butadiene oxidation.

bond in the initial autoxidation product will produce highly reactive free radicals. Then, the generated free radicals can react with peroxides or 1,3-butadiene to form complex products. Rapid oxidation reactions must be avoided because they can lead to runaway reactions or explosion hazards.

The other pathway is the dimerization of 1,3-butadiene. Dimerization of 1,3-butadiene through Diels-Alder type cycloaddition was suggested based on previous work (Doering et al., 1972; Berson and Dervan, 1973) to predict a reaction mechanism. Two isomers of 1,3-butadiene, *cis*-1,3-butadiene and *trans*-1,3-butadiene, would dimerize into 4-vinylcyclohexane, 1,5-cyclooctadiene, *trans*-1,2-divinylcyclobutane, and *cis*-1,2-divinylcyclobutane dimers. These reactions would take place through the formation of the intermediate octa-1,7-diene-3,6-diyl diradicals (*trans*, *trans*), (*cis*, *trans*), and (*cis*, *cis*) (Aldeeb et al., 2004). In the presence of abundant O_2, 4-vinylcyclohexane and 1,5-cyclooctadiene would oxidize into 3-cyclohexene-1-carboxaldehyde, 3-cyclohexene-1-carboxylic acid, 5,10-dioxatricyclo[7.1.0.0^{4,6}]decane, 9-oxabicyclo[6.1.0]non-4-ene, 2,6-cyclooctadien-1-ol, and 2,6-cyclooctadien-1-one.

4. Conclusion

The oxidation reactions of 1,3-butadiene under oxygen and initiator (including CHP and AIBN) were studied using a self-designed mini closed pressure vessel test (MCPVT) technology. This work would be of great interest to continue studying the hydroperoxides formed during the low-temperature oxidation of an organic compound. The following conclusions were obtained:

(1) *T-t*, *P*-t, and *n-t* curves suggest that 1,3-butadiene had a significant oxidation reaction when the temperature was 343 K. CHP and AIBN performed prominent exothermic peaks. The initial exothermic temperatures were 394.65 K and 342.28 K, respectively. The system exhibited a remarkably more significant pressure drop in the presence of initiators.

(2) The oxidation kinetics of 1,3-butadiene were studied by pressure versus time in MCPVT. The order for the reaction rate of the three oxidation models was CHP-initiated, AIBN-initiated, and autoxidation. The activation energies of autoxidation, CHP-initiated oxidation, and AIBN-initiated oxidation reaction were 20.85 kJ·mol^{-1}, 33.30 kJ·mol^{-1}, and 56.27 kJ·mol^{-1}, respectively.

(3) The effect of the main reaction conditions (reaction time, temperature, the molar ratio of 1,3-butadiene-to-oxygen, and initiators) on the peroxide value of the oxidation reaction was investigated. The results showed that 1,3-butadiene was vital for peroxide production in contact with oxygen and tended to proceed with the decomposition of peroxide to form oxidation products.

(4) The thermal decomposition characteristics of oxidation products were determined by DSC. In an autoxidation model, its decomposition heat was increased with an increasing peroxide value, indicating that peroxide is a highly hazardous substance. The residual initiator would widen the exothermic peak and increase the exothermic heat.

(5) The gas, liquid, and volatile components in solid state products were formed in the three oxidation models reaction. The oxidation of 1,3-butadiene may yield, more or less, the same set of oxidized products. Additional products may derive from subsequent cleavage or addition reactions of intermediate species depending on the conditions.

In summary, it is expected that this study of the oxidation of 1,3-butadiene under different conditions will significantly facilitate the interpretation of thermal stability and safety of 1,3-butadiene. It may thus provide greater insight into understanding their thermal characteristics and avoiding accidents in production, transportation, and application.

5. Availability of data and materials

All data generated or analyzed during this study are included in this published article.

Declaration of Competing Interest

The authors declare that they have no known competing financial interests or personal relationships that could have appeared to influence the work reported in this paper.

Acknowledgements

This work was supported by the National Natural Science Foundation of China, China (21776050), National Institute of Advanced Industrial Science and Technology Fellowship of Japan, Major Science and Technology Special Project in Guangxi, China (AA17204087-20), Innovation training program of Guangxi Zhuang Autonomous Region (R2030042001).

Authors' contributions

C.Y., F.L., and W.L. contributed to the method design and equipment improvement. M.L., S.D., H.Z., and H.C. performed the experiments and collected data. M.L., L.M., and X.L. coordinated the study and wrote the manuscript. All authors gave final approval for publication.

Funding

Major Science and Technology Special Project in Guangxi, AA17204087-20.

National Natural Science Foundation of China, 21776050.

National Institute of Advanced Industrial Science and Technology Fellowship of Japan

References

Abdollahi, M., Hajiataloo, M.A., 2021. Radical polymerization of butadiene mediated by molecular iodine: A comprehensive kinetic study on solution copolymerization with acrylonitrile. Polymer 214, https://doi.org/10.1016/j.polymer.2020.123255 123255.

Adusei, G.Y., Fontijn, A., 1993. Kinetics of the reaction between oxygen (3P) atoms and 1,3-butadiene between 280 and 1015 K. J. Phys. Chem. 97, 1406–1408. https://doi.org/10.1021/j100109a025.

Aldeeb, A.A., Rogers, W.J., Mannan, M.S., 2004. Evaluation of 1,3-butadiene dimerization and secondary reactions in the presence and absence of oxygen. J. Hazard. Mater. 115, 51–56. https://doi.org/10.1016/j.jhazmat.2004.06.019.

Alexander, D.S., 1959. Explosions in Butadiene Systems. Ind. Eng. Chem. 51, 733–738. https://doi.org/10.1021/ie50594a026.

Assa, L., Menashe, B., 1989. Thermal reactions of cyclic ethers at high temperatures. 5. Pyrolysis of 2,3-dihydrofuran behind reflected shocks. J. Phys. Chem. B 93, 1139–1144. https://doi.org/10.1021/j100340a024.

Assa, L., Menashe, B., Shimon, B., 1986. Thermal reactions of cyclic ethers at high temperatures. 4. Pyrolysis of 2,5-dihydrofuran behind reflected shocks. J. Phys. Chem. B 90, 6011–6014. https://doi.org/10.1021/j100280a110.

Berson, J.A., Dervan, P.B., 1973. Mechanistic analysis of the four pathways in the 1,3-sigmatropic rearrangements of trans-1,2-trans, trans- and trans-1,2-cis, trans-dipropenylcyclobutane. J. Am. Chem. Soc. 95, 269–270. https://doi.org/10.1021/ja00782a062.

Bonnevide, M., Phan, T., Malicki, N., Kumar, S.K., Jestin, J., 2020. Synthesis of polyisoprene, polybutadiene and Styrene Butadiene Rubber grafted silica nanoparticles by nitroxide-mediated polymerization. Polymer 190,. https://doi.org/10.1016/j.polymer.2020.122190 122190.

Brezinsky, K., Burke, E.J., Glassman, I., 1985. The high temperature oxidation of butadiene. Symp. (Int.) Combust. 20, 613–622 https://doi.org/10.1016/S0082-0784(85)80550-6.

Cavani, F., Centi, G., Trifiro, F., 1983. Oxidation of 1-butene and butadiene to maleic anhydride. 2. Kinetics and mechanism. Ind. Eng. Chem. Prod. Res. Dev. 22, 570–577. https://doi.org/10.1021/i300012a011.

Chen, K.Y., Wu, S.H., Wang, Y.W., Shu, C.M., 2008. Runaway reaction and thermal hazards simulation of cumene hydroperoxide by DSC. J. Loss Prev. Process Ind. 21, 101–109 https://doi.org/10.1016/j.jlp.2007.09.002.

Colket, M.B., Naegeli, D.W., Glassman, I., 1977. High Temperature Oxidation of Acetaldehyde. Symp. (Int.) Combust. 16, 1023–1039. https://doi.org/10.1016/S0082-0784(77)80393-7.

Crawford, R.J., Lutener, S.B., Cockcroft, R.D., 1976. The thermally induced rearrangements of 2-vinyloxirane. Can. J. Chem. 54, 3364–3376. https://doi.org/10.1139/v76-484.

Dai, L., Wang, X., Bu, Z., Li, B., Jie, S., 2019. Facile access to carboxyl-terminated polybutadiene and polyethylene from *cis*-polybutadiene rubber. J. Appl. Polym. Sci. 136, 46934. https://doi.org/10.1002/app.46934.

Denisov, E.T., Denisova, T.G., Pokidova, T.S., 2003. Handbook of Free Radical Initiators. Wiley-Interscience 591–653. https://doi.org/10.1002/0471721476.

Dias, M.L., Schoene, F., Ramirez, C., Graciano, I.A., Gonalves, R.P., 2019. Thermal and crystallization behaviour of epoxidized high *cis*-polybutadiene rubber. J. Rubber Res. 22, 195–201. https://doi.org/10.1007/s42464-019-00028-5.

Doering, W. von E., Franck-Neumann, M., Hasselmann, D., Kaye, R. L., 1972. Mechanism of a Diels-Alder reaction. Butadiene and its dimers. J. Am. Chem. Soc. 94, 3833–3844. https://doi.org/10.1021/ja00766a029.

Feng, Y., Zeng, A., 2020. Selective Liquid-Phase Oxidation of Toluene with Molecular Oxygen Catalyzed by Mn3O4 Nanoparticles Immobilized on CNTs under Solvent-Free Conditions. Catalysts 10, 623. https://doi.org/10.3390/catal10060623.

Ghosh, B., Bugarin, A., Connell, B.T., North, S.W., 2010a. OH Radical Initiated Oxidation of 1,3-Butadiene: Isomeric Selective Study of the Dominant Addition Channel. J. Phys. Chem. A 114, 5299–5305. https://doi.org/10.1021/jp1006878.

Ghosh, B., Park, J., Anderson, K.C., North, S.W., 2010b. OH initiated oxidation of 1,3-butadiene in the presence of O_2 and NO. Chem. Phys. Lett. 494, 8–13 https://doi.org/10.1016/j.cplett.2010.05.056.

Guilun, W., Jijiang, F., Jie, L., 2013. Butadiene Popcorn Polymer Resource Book. Chemical Industry Press, Beijing.

Handy, C.T., Rothrock, H.S., 1958. Polymeric Peroxide of 1,3-Butadiene. J. Am. Chem. Soc. 80, 5306–5308. https://doi.org/10.1021/ja01552a075.

Hendry, D.G., Mayo, F.R., Jones, D.A., Schuetzle, D., 1968a. Stability of Butadiene Polyperoxide. Ind. Eng. Chem. Prod. Res. Dev. 7, 145–151. https://doi.org/10.1021/i360026a011.

Hendry, D.G., Mayo, F.R., Schuetzle, D., 1968b. Oxidation of 1,3-butadiene. Ind. Eng. Chem. Prod. Res. Dev. 7, 136–145. https://doi.org/10.1021/i360026a010.

Hsu, J.M., Su, M.S., Huang, C.Y., Duh, Y.S., 2012. Calorimetric studies and lessons on fires and explosions of a chemical plant producing CHP and DCPO. J. Hazard. Mater. 217–218, 19–28 https://doi.org/10.1016/j.jhazmat.2011.12.064.

Huang, N.J., Sundberg, D.C., 1995. Fundamental studies of grafting reactions in free radical copolymerization. IV. Grafting of styrene, acrylate, and methacrylate monomers onto vinyl-polybutadiene using benzoyl peroxide and AIBN initiators in solution polymerization. J. Polym. Sci. Part A: Polym. Chem. 33, 2587–2603. https://doi.org/10.1002/pola.1995.080331505.

Klais, O., 1993. Hydrogen peroxide decomposition in the presence of organic material: A case study. Thermochim Acta 225, 213–222. https://doi.org/10.1016/0040-6031(93)80189-H.

Kramp, F., Paulson, S.E., 2000. The gas phase reaction of ozone with 1,3-butadiene: formation yields of some toxic products. Atmos. Environ. 34, 35–43. https://doi.org/10.1016/S1352-2310(99)00327-1.

Li, Z., Nguyen, P., Fatima de Leon, M., Wang, J.H., Han, K., He, G. Z., 2006a. Experimental and Theoretical Study of Reaction of OH with 1,3-Butadiene. J. Phys. Chem. A 110, 2698–2708. https://doi.org/10.1021/jp0556557.

Li, Z., Nguyen, P., Maria, F., Wang, J.H., Han, K., He, G.Z., 2006b. Experimental and Theoretical Study of Reaction of OH with 1;3-Butadiene. J. Phys. Chem. A 110, 2698–2708. https://doi.org/10.1021/jp0556557.

Li, Y., Xu, X., Niu, M., Chen, J., Liu, X., 2019. Thermal Stability of Abietic Acid and Its Oxidation Products. Energy Fuels 33. https://doi.org/10.1021/acs.energyfuels.9b02855.

Lifshitz, A., Laskin, A., 1994. Isomerization of 2Methyl4,5-dihydrofuran. Studies with a Single-Pulse Shock Tube. J. Phys. Chem. 98, 2341–2345. https://doi.org/10.1021/j100060a023.

Liu, S.H., Lin, C.P., Shu, C.M., 2011. Thermokinetic parameters and thermal hazard evaluation for three organic peroxides by DSC and TAM III. J. Therm. Anal. Calorim. 106, 165–172. https://doi.org/10.1007/s10973-011-1582-x.

Liu, P., Liu, X., Saburi, T., Kubota, S., Wada, Y., 2020. Thermal characteristics and hazard of 1,3-Butadiene (BD) polymerization and oxidation. Thermochim Acta 178713. https://doi.org/10.1016/j.tca.2020.178713.

Liu, A., Mulac, W.A., Jonah, C.D., 1988. Rate constants for the gas-phase reactions of hydroxyl radicals with 1,3-butadiene and allene at 1 atm in argon and over the temperature range 305–1173 K. J. Phys. Chem. 92, 131–134. https://doi.org/10.1021/j100312a028.

Liu, S.H., Yu, C.F., Das, M., 2019. Thermal hazardous evaluation of autocatalytic reaction of cumene hydroperoxide alone and mixed with products under isothermal and non-isothermal conditions. J. Therm. Anal. Calorim. 140, 2325–2336. https://doi.org/10.1007/s10973-019-09017-7.

Mayo, F.R., 1958. The Oxidation of Unsaturated Compounds. V. The Effect of Oxygen Pressure on the Oxidation of Styrene 1,2. J. Am. Chem. Soc. 80, 2465–2480. https://doi.org/10.1021/ja01543a030.

Mayo, F.R., Miller, A.A., Russell, G.A., 1957. The Oxidation of Unsaturated Compounds. IX. The Effects of Structure on the Rates and Products of Oxidation of Unsaturated Compounds1,*. J. Am. Chem. Soc. 80, 2500–2507. https://doi.org/10.1021/ja01543a034.

Mettler, T., 2004. STAR^{e} Software with Solaris Operating System.

Okada, K., Ai, F., Akiyoshi, M., Shu, U., Matsunaga, T., 2014. Thermal hazard evaluation of ammonium nitrate emulsions by DSC and 1.5 L pressure vessel test. Sci. Technol. Energetic Mater. 75, 1–7.

Paz-Pazos, M., Pugh, C., 2005. Synthesis, isolation, and thermal behavior of polybutadiene grafted with poly(2,3,4,5,6-pentafluorostyrene). J. Polym. Sci., Part A: Polym. Chem. 43, 2874–2891. https://doi.org/10.1002/pola.20765.

Persson, P.A., Holmberg, R., Jaimin, L., 2018. United Nations Recommendations on the Transport of Dangerous Goods. Rock Blasting and Explosives Engineering.

Ren, F., Zheng, Y.F., Liu, X.M., Yang, Q.Q., Zhang, Q., Shen, F., 2015. Thermal oxidation reaction process and oxidation kinetics of abietic acid. RSC Adv. 5, 17123–17130. https://doi.org/10.1039/c4ra16791k.

Robey, R.F., Wiese, H.K., Morrell, C.E., 1944. Stability of Butadiene. Ind. Eng. Chem. 36, 3–7. https://doi.org/10.1021/ie50409a002.

Safa, M.A., Ma, X., 2015. Oxidation kinetics of dibenzothiophenes using cumene hydroperoxide as an oxidant over MoO3/Al2O3 catalyst. Fuel 171, 238–246. https://doi.org/10.1016/j.fuel.2015.12.050.

Vasu, S.S., Zádor, J., Davidson, D.F., Hanson, R.K., Golden, D.M., Miller, J.A., 2010. High-Temperature Measurements and a Theoretical Study of the Reaction of OH with 1,3-Butadiene. J. Phys. Chem. A. 114, 8312–8318. https://doi.org/10.1021/jp104880u.

Vuppaladadiyam, A.K., Liu, H., Zhao, M., Soomro, A.F., Memon, M.Z., Dupont, V., 2019. Thermogravimetric and kinetic analysis to discern synergy during the co-pyrolysis of microalgae and swine manure digestate. Biotechnol. Biofuels 12, 170. https://doi.org/10.1186/s13068-019-1488-6.

Wang, R., Liu, D., Li, X., Zhang, J., Cui, D., Wan, X., 2016. Synthesis and Stereospecific Polymerization of a Novel Bulky Styrene Derivative. Macromolecules 49, 2502–2510. https://doi.org/10.1021/acs.macromol.6b00325.

Wang, B., Liu, X.M., Fu, X.N., Li, Y.L., Huang, P.X., Zhang, Q., Li, W.G., Ma, L., Lai, F., Wang, P.F., 2018. Thermal stability and safety of dimethoxymethane oxidation at low temperature. Fuel 234, 207–217 https://doi.org/10.1016/j.fuel.2018.07.034.

Wellington, C.A., Walters, W.D., 2012. The Vapor Phase Decomposition of 2,5-Dihydrofuran. J. Am. Chem. Soc. 83, 4888–4891. https://doi.org/10.1021/ja01485a004.

Wu, S.H., Chou, H.C., Pan, R.N., Huang, Y.H., Horng, J.J., Chi, J. H., Shu, C.M., 2012a. Thermal hazard analyses of organic peroxides and inorganic peroxides by calorimetric approaches. J. Therm. Anal. Calorim. 109, 355–364. https://doi.org/10.1007/s10973-011-1749-5.

Wu, S.H., Wu, J.Y., Wu, Y.T., Lee, J.C., Huang, Y.H., Shu, C.M., 2012b. Explosion evaluation and safety storage analyses of cumene hydroperoxide using various calorimeters. J. Therm. Anal. Calorim. 111, 669–675 https://doi.org/10.1007/s10973-012-2570-5.

Yamamoto, T., Takahashi, Y., 2016. Synthesis of Hydrocolloid through Polymerization of Styrene and N-Vinyl Acetamide by AIBN. Colloids Surf. A 516, 80–84. https://doi.org/10.1016/j.colsurfa.2016.12.023.

You, M.L., Tseng, J.M., Shu, L.C.M., 2010. Runaway reaction of lauroyl peroxide with nitric acid by DSC. J. Therm. Anal. Calorim. 102, 535–539. https://doi.org/10.1007/s10973-010-0934-2.

Zhang, C.X., Lu, G.B., Chen, L.P., Chen, W.H., Peng, M.J., Lv, J.Y., 2015. Two decoupling methods for non-isothermal DSC results of AIBN decomposition. J. Hazard. Mater. 285, 61–68. https://doi.org/10.1016/j.jhazmat.2014.11.022.

Zhang, Z., Mamba, T., Huang, Q.A., Murayama, H., Yamamoto, E., Honma, T., Tokunaga, M., 2019. The additive effect of amines on the dihydroxylation of buta-1,3-diene into butenediols by supported Pd catalysts. Mole. Catal. 475, 110502 https://doi.org/10.1016/j.mcat.2019.110502.